nature methods

Perspective

https://doi.org/10.1038/s41592-023-02041-4

Artificial intelligence-enabled quantitative phase imaging methods for life sciences

Received: 25 February 2023

Accepted: 11 September 2023

Published online: 23 October 2023

Check for updates

Juyeon Park[1,2,9], Bijie Bai[3,4,9], DongHun Ryu[1,2,8], Tairan Liu[3], Chungha Lee[1,2], Yi Luo[3], Mahn Jae Lee[2,5], Luzhe Huang[3], Jeongwon Shin[2,6], Yijie Zhang[3], Dongmin Ryu[7], Yuzhu Li[3], Geon Kim[1,2], Hyun-seok Min[7], Aydogan Ozcan[3,4] & YongKeun Park[1,2,7]

Quantitative phase imaging, integrated with artificial intelligence, allows for the rapid and label-free investigation of the physiology and pathology of biological systems. This review presents the principles of various two-dimensional and three-dimensional label-free phase imaging techniques that exploit refractive index as an intrinsic optical imaging contrast. In particular, we discuss artificial intelligence-based analysis methodologies for biomedical studies including image enhancement, segmentation of cellular or subcellular structures, classification of types of biological samples and image translation to furnish subcellular and histochemical information from label-free phase images. We also discuss the advantages and challenges of artificial intelligence-enabled quantitative phase imaging analyses, summarize recent notable applications in the life sciences, and cover the potential of this field for basic and industrial research in the life sciences.

Optical imaging techniques have been indispensable tools for investigating living systems for many centuries. The ability to image biological systems in high resolution over space and time would allow us to reveal the morphology and dynamics of these systems, providing insights into their underlying mechnisms[1]. Across various biological imaging techniques, quantitative phase imaging (QPI) methods have rapidly emerged as powerful tools[2–5]. QPI methods take advantage of high-speed, three-dimensional (3D) imaging of living organisms at subcellular resolution in a nondestructive and label-free manner. As QPI methods exploit refractive index (RI) as an endogenous imaging contrast, they do not require exogenous labels for specimens, making them free from labeling-induced issues such as photobleaching, toxicity and variable data quality.

Alongside the growing utility of QPI methods in biomedicine, recent breakthroughs in artificial intelligence (AI) algorithms have expanded the capability and applicability of QPI methods. These breakthroughs have enabled fast and accurate downstream tasks such as image enhancement, classification, segmentation and translation of biomedical data (Fig. 1). In particular, the performance of deep learning approaches has been unprecedented, with the ability to approximate complex nonlinear functions for image processing tasks[6]. This has offered versatile solutions to numerous challenges in bioimaging. The quantitative and uniform-quality data generated by QPI methods enable deep learning approaches to efficiently learn target tasks and provide robust analysis tools for new biological discoveries.

In this Review, we focus on the integration of QPI and AI and how this intersection has advanced biomedical research. We introduce the principles, advantages and implementations of QPI methods, highlight the biomedical applications that have been achieved through this

[1]Department of Physics, Korea Advanced Institute of Science and Technology (KAIST), Daejeon, Republic of Korea. [2]KAIST Institute for Health Science and Technology, KAIST, Daejeon, Republic of Korea. [3]Electrical and Computer Engineering Department, University of California, Los Angeles, Los Angeles, CA, USA. [4]Bioengineering Department, University of California, Los Angeles, Los Angeles, CA, USA. [5]Graduate School of Medical Science and Engineering, Korea Advanced Institute of Science and Technology (KAIST), Daejeon, Republic of Korea. [6]Department of Biological Sciences, Korea Advanced Institute of Science and Technology (KAIST), Daejeon, Republic of Korea. [7]Tomocube, Daejeon, Republic of Korea. [8]Present address: Department of Electrical Engineering and Computer Science, Massachusetts Institute of Technology, Cambridge, MA, USA. [9]These authors contributed equally: Juyeon Park, Bijie Bai. e-mail: ozcan@ucla.edu; yk.park@kaist.ac.kr

https://doi.org/10.1038/s41592-023-02041-4

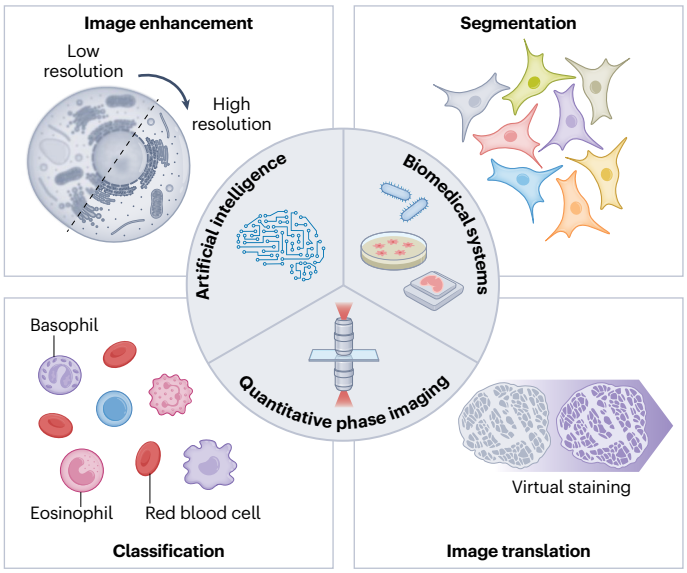

Fig. 1 | AI-integrated QPI methods applied to biomedical research. Synergistic combination of AI and QPI techniques can be applied to various biomedical research areas, including image enhancement, segmentation, classification and translation.

combination and discuss the outlook for this emerging synergy in the areas of systems biology and digital medicine.

QPI

Principles of QPI

When light passes through a transparent object, its phase, rather than its amplitude, is primarily modulated. However, as most biological systems are inherently transparent, it is challenging to obtain high-quality images using conventional bright-field microscopy, which can only measure the intensity of the light transmitted from a sample. Utilizing the phase as an imaging contrast can provide a solution to visualize transparent systems, but the phase cannot be directly measured using standard image sensors, as the bandwidth of modern imagers is yet to be sufficiently high to record the phase with high temporal frequency. To circumvent this limit, Zernike's phase contrast microscopy[7] and its variants[8] have been developed. They introduce a phase plate in an optical imaging system, which enables the conversion of the modulated phase into detectable intensity contrast, allowing visualization of the phase modulation induced by the transparent samples. However, the nonlinear relationship between the phase and the measured intensity limits their use to qualitative analysis of biological systems.

To overcome the qualitative nature of Zernike's phase contrast microscopy, various QPI methods have been developed to achieve quantitative analyses of biological systems (Fig. 2a–c). QPI methods can generally be categorized into either interferometric or non-interferometric QPI (Fig. 2a,b). Interferometric QPI methods utilize the interference between a sample beam, scattered from a sample, and a reference beam. Both beams are recorded as an interferogram, from which both the amplitude and phase images are retrieved using field retrieval algorithms[2,9–11]. On the contrary, non-interferometric QPI methods reconstruct the amplitude and phase information from the transmitted intensity images obtained under specific illumination or imaging conditions[12,13]. The phase images are then retrieved from the intensity images using intensity and phase relations, which vary with the type of QPI method used[14–16]. It should be noted that the term 'non-interferometric' is introduced to clearly differentiate it from the use of an interferogram to retrieve phase. However, the basic principle of image formation based on the interference between incident and scattered waves is still valid[17].

Advantages of using QPI for biomedical applications

To understand the advantages of QPI approaches for biological studies, it is helpful to compare them with other standard imaging methods, such as fluorescence microscopy and phase contrast microscopy (Fig. 2d). Fluorescence microscopy is a cornerstone method for visualizing various cellular and subcellular components of living biological systems. By using fluorescent probes that label specific molecules within cells, it is possible to simultaneously visualize various target system components, such as proteins and lipids, and their associated pathophysiology with high specificity and signal-to-noise ratio. However, preparing fluorescence-labeled samples can be a labor-intensive procedure, as overnight transfection of fluorescent protein reporters or other time-consuming serial procedures must precede imaging. Moreover, photobleaching and phototoxicity severely limit the available time over which a sample can be observed by fluorescence microscopy. Continuous exposure to light from fluorescence microscopy can damage fluorescent molecules and make them gradually lose their ability to fluoresce, a phenomenon known as photobleaching[18]. In addition, cells are susceptible to phototoxicity, which is enhanced by the reactive chemical species generated by fluorescent molecules under illumination[19]. Recent advances in fluorescence microscopy techniques, such as light-sheet microscopy[20,21], two-photon microscopy[22,23], total internal reflection fluorescence microscopy[24,25] and their integration with QPI techniques[26], have mitigated photobleaching and phototoxicity by reducing the out-of-plane exposure[27]. However, the fundamental issues associated with labeling remain, highlighting the need for label-free imaging in various biological and life science-related applications.

Phase contrast microscopy has been widely adopted in biological studies because it allows researchers to easily obtain high-contrast images of unlabeled specimens by converting phase shifts, induced by a transparent specimen, to amplitude variations. However, phase contrast microscopy can only measure thin specimens in two dimensions (2D)[7]. To obtain volumetric information, it is common to manually scan the sample along the optical axis. Importantly, the qualitative nature of both fluorescence microscopy and phase contrast microscopy can restrict one from performing consistent analysis. Calibration challenges originating from different users and variables in the protocols and imaging systems could produce inconsistent and irreproducible experimental results.

Compared to these conventional approaches, there are unique benefits to using QPI methods for biomedicine. First, QPI approaches that do not require fixations or labeling enable the continual monitoring of cells and tissues. For example, QPI can be used for long-term monitoring of neuronal morphology without any interventions once the sample is prepared[28]. Rapid medical tests could also be realized by the short turnaround time of label-free QPI approaches[29,30]. Early screening of acute diseases, such as sepsis[31], is crucial for their diagnosis and treatment. QPI-based testing frameworks could provide suitable solutions for rapid screening. In addition, its ability to image intact cells would be crucial in various clinical research studies where unmodified cells or tissues that are transplantable to patients could be important.

In addition to the label-free imaging capability, QPI provides various morphological and biochemical parameters quantitatively, enabling systematic and statistical analysis at the single-cell level. It has been extensively studied that the RI distribution and its associated quantitative phase map of the specimen are directly related to characteristic parameters, such as cell volume, surface area, sphericity and dry mass, which corresponds to the nonaqueous content of the cells[5,32,33]. By harnessing these multidimensional parameters generated using QPI methods, one may find unexplored insights and interpretations of

https://doi.org/10.1038/s41592-023-02041-4

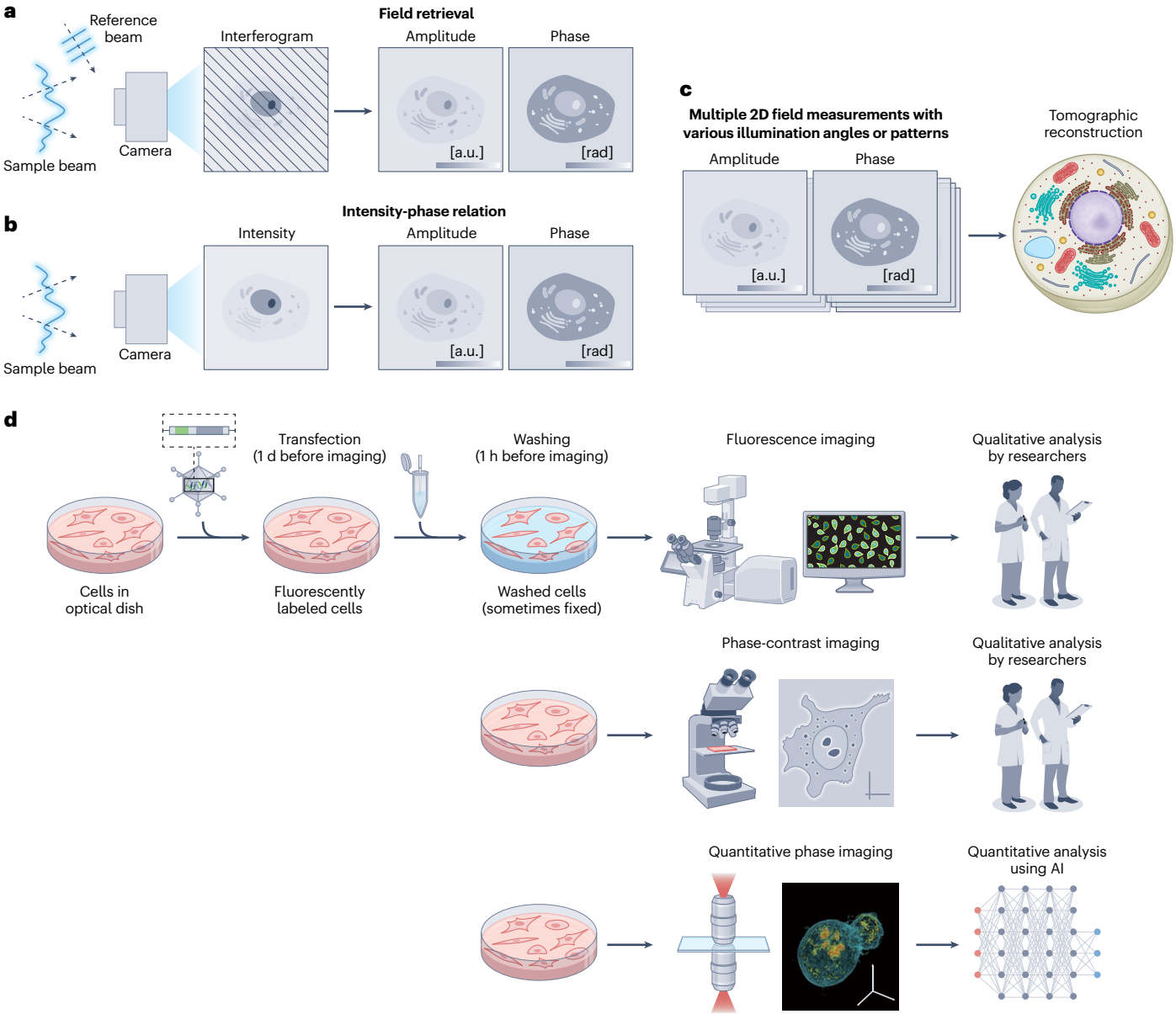

Fig. 2 | Principles and advantages of QPI. a,**b**, Schematics of the principles of interferometric and non-interferometric QPI methods. Interferometric QPI methods measure interference patterns between a sample and reference beams, or interferograms, while non-interferometric QPI methods capture transmitted intensity images. Depending on the type of QPI method, either field retrieval or intensity–phase relations are used to reconstruct phase images of the specimen. **c**, Schematic of tomographic reconstruction of QPI methods, achieving 3D visualization of biomedical systems. **d**, Advantages of using machine learning-integrated QPI for life science-related studies. Compared to conventional fluorescence imaging, QPI methods do not require staining or labeling before imaging, resulting in quantitative measurements and facilitating the integration of machine learning for robust downstream analyses. a.u., arbitrary units.

biological experiments with computational analysis. We also envision that present-day AI algorithms and graphic processing units that can process a massive amount of data would enable large-scale QPI data to be analyzed, creating new possibilities in biomedical research.

Implementations of QPI

The essence of QPI was established by Gabor in 1948 when he proposed an imaging strategy for correcting the spherical aberrations of electron lenses[34]. By measuring the interference pattern between the illumination wave and the secondary wave scattered from an object at an out-of-focus position, 'a complete record of amplitudes and phases' of the scattered field became possible. The early QPI techniques of this type, such as the Gabor in-line holography, have been extensively explored by researchers[35–37]. The implementations of in-line holography often use phase-shifting interferometry, which retrieves the quantitative phase distribution of a sample from multiple measurements obtained with different phase shifts introduced to the reference beam. However, this method requires at least four sequentially captured phase-shifted images[35–37], which limits the throughput of the systems.

Furthermore, as Gabor pointed out, in-line holography is incapable of 'distinguishing positive and negative phase shifts' with respect to illuminating waves along the optical axis. As a result of recording

https://doi.org/10.1038/s41592-023-02041-4

only the intensity of a hologram, it also generates twin images of the same amount of phase shifts but with reversed signs[34]. A straightforward strategy to address this issue is the spatial separation of the twin images at the Fourier space, which can be realized by the angular separation of the reference beam from the sample beam[38], that is, using off-axis configuration[39]. Notably, off-axis holography not only allows the physical separation of the twin images but also requires only one single hologram to uniquely determine the phase of the scattered field. Such single-shot imaging capability becomes crucial when monitoring the dynamics of moving objects, namely, living cells, in real time. For such merit, various QPI techniques have been developed based on the off-axis geometry, including digital holographic microscopy[9], Hilbert phase microscopy[11] and diffraction phase microscopy[10].

QPI methods in general have used coherent light sources. However, the use of coherent sources poses a fundamental challenge to the accurate reconstruction of scattered fields: the coherence of the light source might generate excessive interference fringes due to scattered light from unwanted objects (for example, dust particles or surface scratches) within the sample volume. To manage and suppress coherence artifacts and noise, numerous efforts have been made in developing partially coherent or incoherent QPI methods. Examples include spatial light interference microscopy (SLIM)[40] and white-light diffraction phase microscopy[41], which modulate the reference beam temporally and spatially, respectively, to obtain phase images. In addition to noise reduction, these approaches can also enable a higher space–bandwidth product, such as in Fourier ptychographic microscopy (FPM)[16,42] and differential phase contrast microscopy[15,43]. FPM combines multiple low-resolution images captured under different illumination angles to produce a high-resolution phase image over a large field of view, whereas differential phase contrast microscopy recovers phase images from measurements under asymmetric illumination patterns. Additional examples include quadriwave lateral shearing interferometry[44] and gradient light interference microscopy[45], which can be easily integrated into conventional optical microscopes for QPI. Furthermore, lens-free on-chip holography[46–49] with partially coherent illumination light has also been developed, which achieves a very large sample volume to be probed in a compact optical setup. A special case of non-interferometric QPI is based on the transport of intensity equation (TIE), which relates the axial derivative of the optical intensity to the phase information of the sample at the in-focus plane[50,51]. Therefore, to extract the phase information of the sample using TIE, axial scanning of a sample is necessary[12].

Further advances have been made over the past few decades to develop QPI methods for 3D samples[52,53], which have been extensively utilized in biological research[54–57]. Among those, optical diffraction tomography (ODT), theoretically introduced in 1969 (ref. 58), achieves reconstruction of the 3D RI map of a sample. The reconstruction is based on multiple 2D fields retrieved from 2D holograms of the sample illuminated at various angles[3]. Furthermore, ODT that uses a partially coherent source has also been demonstrated[13,59–62]. Other efforts have been made to solve the multiple scattering problems, which occur when the first Born approximation is no longer valid for optically thick samples[63–66]. Additionally, flow cytometric strategies are combined with digital holography, enabling high-throughput 3D imaging of individual cells[67]. The commercialized QPI techniques are shown in Table 1.

Recent QPI methods have addressed diverse imaging challenges across cellular to tissue scales. At the cellular scale, the label-free 3D imaging capability of ODT has enabled the monitoring of neurite growth[28] and provided biomechanical insights by measuring the 3D traction forces of individual cells[68]. The low spatial noise and temporal stability of SLIM allowed it to be used to quantify the cell-to-cell lipid-content heterogeneity[69] and study microtubule motility[70]. Furthermore, QPI methods were used to address tissue-level challenges, such as monitoring vasculogenesis and the measurement of microvascular permeability[71], structural heterogeneity[72] and stiffness[73] of tissue. As QPI methods continue to improve and overcome technical limitations, they can address future challenges in life science-related imaging needs, including imaging freshly excised tissue samples and performing in vivo, intraoperative and organ-level imaging.

Table 1 | Commercialized QPI techniques and their applications

Manufacturers	Technique (product)	Applications
Trimos	White-light interferometry[9] (TR scan series)	Surface topography
Holmarc	Digital holographic microscopy[9] (HO series)	Cancer cell biology, particle detection
Lyncée Tec	Digital holographic microscopy[9] (DHM series)	Cytotoxicity, cell dynamics, neuroscience, surface topography, dynamic topography
Phasics	Quadriwave lateral shearing interferometry[44] (SID4 series)	Cytology, histology, surface topography
PHI AB	Digital holographic microscopy[9] (HoloMonitor)	Cell motility, cell migration, wound healing, 3D matrix cell culture assays
Telight	White-light digital holographic microscopy[9] (Q-Phase)	Cancer cell biology, immunology, drug toxicity, 3D matrix cell culture assays
Nanolive	Holographic tomography[3] (3D cell explorer series)	Cytotoxicity, intercellular dynamics, lipid imaging, cancer cell biology
Phasefocus	Ptychogarphic QPI[174] (LiveCyte)	Wound healing, angiogenesis, toxicology
Phi Optics	White-light diffraction phase microscopy (ref. 41)[a], SLIM (ref. 40)[a], gradient light interference microscopy (ref. 45)[a]	Cell topography, cell dynamics, cell growth, neuroscience, tissue imaging, developmental biology
Tomocube	The 1st generation holotomography (HT-2)[3] The 2nd generation holotomography (HT-X1)[14,61,175]	Cell therapy, organoid imaging and analysis, intercellular dynamics, lipid imaging, bacteria analysis
Lucendi	In-line holography[46] (Aqusens)	In-field, automated monitoring of micro-objects in liquids
Spheryx	In-line holography[46] (total holographic characterization)	Cell viability, pharmaceutical monitoring, screening semiconductor and water quality
Conzeb	Free-space angular-chirp-enhanced delay[176–178] (FACED)	Blood screening, cancer cell biology, imaging flow cytometry

[a]Add-on module

The combination of AI and QPI

QPI methods have been beneficial in a wide array of biomedical domains, owing to the capability of extending to 3D imaging and extracting diverse biophysical variables. In addition, the reproducible and consistent QPI data invariant across samples and instruments have made AI algorithms more suitable for deployment. Concurrently, the accessibility of AI software infrastructures has led to the widespread adoption of AI algorithms in various disciplines, including QPI-based biomedical studies[74–76].

AI algorithms can be applied to diverse phase image reconstruction methods for QPI and subsequent image quality enhancement procedures, allowing scientists to generate data and results accurately and rapidly. In particular, deep neural networks can be actively

Table 2 | AI methods and applications

Learning type	Name	Applications
Machine learning	KNN	Cell classification[132]
	Linear discriminant analysis	Cell classification[143]
	Random forest	Tissue region segmentation[115], cell classification[140]
	SVM	Cell classification[133,134,144,145]
Deep learning/supervised	Contextual aggregation network	Holographic reconstruction[86]
	DenseNet	Bacterial species classification[30], plaque-forming unit classification[151], bacterial colony classification[147]
	Fourier imager network	Holographic reconstruction[85]
	FishNet	Cell classification[29]
	GAN	Holographic reconstruction[80,87], virtual staining[152,154]
	Residual network (ResNet)	Phase unwrapping[88], noise reduction[103], cell classification[138,142,148]
	RNN	Holographic reconstruction[84,100], cell classification[137]
	U-Net	Holographic reconstruction[82,104], Resolution enhancement[89,90,109], noise reduction[101], cellular segmentation[54,55,117–119], virtual staining[57,156]
	Visual geometry group	Tissue region classification[146], cell classification[149]
	Other artificial neural networks (unspecified benchmark)	Holographic reconstruction[79,105], noise reduction[102,107], microalgae classification[141], cell classification[150], cell virtual staining[155]
Deep learning/self-supervised	GedankenNet	Holographic reconstruction[96]
Deep learning/unsupervised	cycleGAN	Holographic reconstruction[92,94], resolution enhancement[95], noise reduction[106], virtual staining[153]
Learning-free/iterative optimization	DIP	Phase reconstruction[98], resolution enhancement[99]

utilized to approximate the phase reconstruction models to improve the speed and quality of reconstructions (further discussed below). Furthermore, a number of image quality enhancement tasks in QPI can benefit from the capacity of deep learning-based methods to model high-dimensional operators, including noise reduction and resolution enhancement. In most cases, these learning-based approaches not only result in reduced image processing time compared to conventional methods[77,78] but also produce more accurate QPI data for computer algorithms and researchers to improve their subsequent analysis.

The rapid and accurate interpretation of QPI images, indispensable for biomedical research, can also be achieved with the help of AI. Some of these tasks include segmentation, classification and cross-modality inference using QPI images. Image segmentation for extracting the region of interest within the target cells or organelles is essential for various tasks, such as cell counting and other biophysical parameter quantification. Conventionally, such segmentations and the following annotations to identify meaningful features are manually performed, which could be labor intensive and inconsistent. AI-assisted segmentation could alleviate these issues, enabling rapid and automated downstream tasks, including object classification and tracking. Furthermore, image classification using AI can enhance the utility of QPI in numerous biological and clinical studies, including rapid classification of cell types and bacterial species.

The superior capability of AI in image-to-image transformation has driven the development of various cross-modality imaging approaches through QPI. AI-enabled cross-modality image-to-image translation from label-free QPI into traditional standard visualizations of biological samples with exogenous labels, such as fluorescence, histochemical and immunohistochemical stains, has provided a nondestructive alternative to inspect biological specimens, which will be further discussed below. Table 2 provides a summary of these algorithms that have been used in QPI for life science applications. Note that the prevailing algorithms reported so far in this field heavily rely on deep learning, which is a subset of AI.

Image reconstruction and enhancement

Conventionally, to determine the quantitative phase information of a sample, iterative reconstruction algorithms are performed to extract phase values from single or multiple intensity-only measurements acquired using sophisticated imaging systems. Some of the major goals for using AI-augmented methods for hologram reconstruction include eliminating the need to use complicated optical systems that require accurate alignment, shortening the data acquisition time and speeding up the phase recovery algorithms.

It has been demonstrated that a deep neural network can be used to quantitatively retrieve the phase distribution of a 2D, thin biological sample measured by different QPI modalities, achieving comparable accuracy to the conventional reconstruction methods[79–81]. For instance, in-line holography has been strengthened by AI[79,82,83]. Rivenson et al.[79] demonstrated using a trained convolutional neural network (CNN) to quantitatively reconstruct the complex optical field from one single intensity measurement using in-line holography (Fig. 3a). The trained CNN also successfully removed the twin image artifact, which normally arises due to the inability of in-line holography to distinguish the sample wave from its complex conjugate using a single hologram, eliminating the need for multiple measurements for the holographic reconstruction. In addition to CNNs, recent studies developed recurrent neural networks (RNNs)[84] and Fourier imager networks[85] for quantitative phase reconstruction using multiple intensity measurements by in-line holography, enabling efficient utilization of sample information encoded in multiple measurements and demonstrating the state-of-the-art reconstruction quality and improved generalization capability among all conventional and AI-based methods. Also, the efficiency of tomographic flow cytometry has been enhanced in terms of processing time and memory by exploiting contextual aggregation networks for the end-to-end reconstruction of RI tomograms[86]. Another emerging QPI technique in recent years, FPM, has also been empowered with AI[80]. By training a neural network, the quantitative phase image can be reconstructed using fewer FPM intensity measurements without compromising the field of view or resolution, which

https://doi.org/10.1038/s41592-023-02041-4

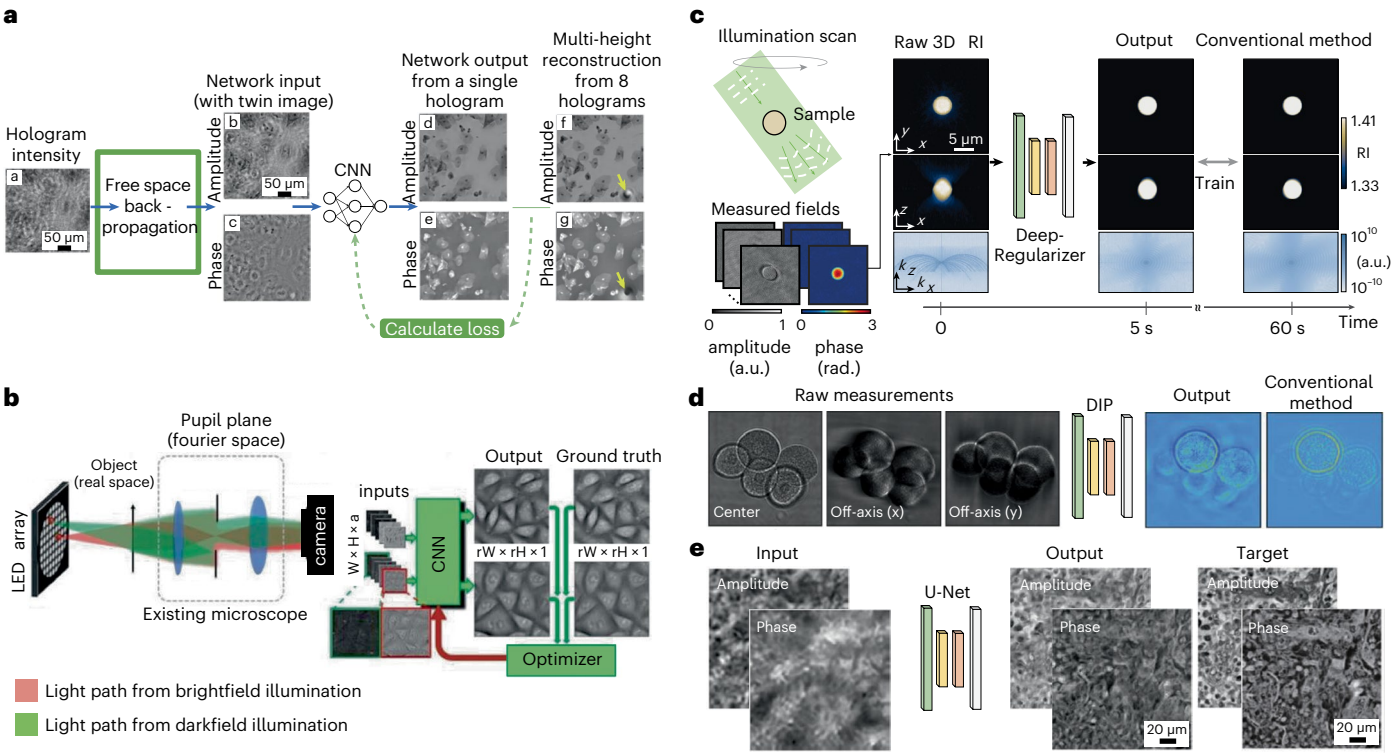

Fig. 3 | Image reconstruction and enhancement of QPI using AI. a,**b**, Use of supervised learning frameworks to reconstruct 2D in-line holography[79] and Fourier Ptychography[80]. **c**, 3D ODT reconstruction using supervised learning[89]. **d**, Iterative optimization methods for reconstructing 3D QPI images with DIP[99]. This method does not have any generalization ability on new samples. **e**, Image enhancement of QPI images using AI, achieving resolution improvement[109].

substantially saves reconstruction time and the required amount of data[80,87] (Fig. 3b). More efforts have also been made in accelerating phase unwrapping[88], which eliminates the 2π ambiguity in the reconstructed phase[88], combining phase recovery with autofocusing, as well as in extending the depth of field of holographic imaging system[82,84]. Besides using AI to improve the QPI reconstruction efficiency or imaging throughput, Wu et al.[83] demonstrated a 'bright-field holography' method, in which a deep neural network was trained to generate volumetric bright-field microscopy images using back-propagation of a single hologram to different positions. It combines the benefits of the high color contrast of bright-field microscopy and the long depth of field of holography, providing a rapid and high-throughput solution to imaging volumetric samples.

Deep learning-based image reconstruction approaches have also been widely used in 3D QPI systems to overcome existing difficulties. One of the challenges is the missing cone problem in diffraction tomography, which refers to the inaccessible information along the z axis of the optical transfer function due to the limited numerical aperture of the objective lens. Conventionally, this problem was addressed by applying regularization algorithms with prior knowledge of the sample properties, for example, non-negativity, low image gradient and so on, and typically requires a long processing time[77]. In this scenario, the data-driven approach can be advantageous in the prediction of missing spatial frequency information and the performance of reconstruction without explicit prior knowledge. Ryu et al.[89] optimized a 3D U-Net that transforms raw RI tomograms of various eukaryotic cells with missing cone artifacts into resolution-enhanced total variation-regularized ones (Fig. 3c). This neural network-based tomogram reconstruction method is more than an order of magnitude faster compared to the conventional iterative methods. Lim et al.[90] created digital phantoms as 3D samples and generated synthetic 2D measurements from the digital phantoms via the discrete dipole approximation. A residual U-Net was trained with this synthetic dataset and successfully reconstructed the 3D tomography of red blood cells using tomograms captured in real experiments.

The abovementioned works fall into the supervised learning category, meaning it requires a comprehensive dataset of well-registered image pairs (for example, a single in-line hologram of a sample and the corresponding phase-recovered image) to train the neural networks. However, under many circumstances, the input image and ground truth image pairs are inaccessible or impractical to obtain. Imperfect registration between the input images and their ground truth labels can also greatly degrade a network's performance. Unsupervised learning methods that do not require paired image dataset have recently gained momentum to tackle this challenge. An unsupervised learning framework termed cycle-consistent generative adversarial networks (cycleGANs)[91] was developed to achieve image-to-image transformation by training two generative adversarial networks (GANs) simultaneously in a cyclic way without using registered image pairs. Researchers demonstrated that, by combining the physical propagation model of light, the cycleGAN framework could be used for QPI reconstruction, replacing conventional iterative methods. For example, Yin et al.[92] demonstrated that the cycleGAN framework could eliminate the aberration artifact better than the traditional principal component analysis-based holographic reconstruction method[93]. Zhang et al.[94] showed a similar framework that outperformed the standard TIE-based phase recovery method. Moreover, the better utility of such a framework is found in situations where ground truth images are challenging to acquire, especially in solving the missing cone artifact for 3D QPI systems. Recently, Chung et al.[95] developed an unsupervised missing cone solver with cycleGANs and experimentally demonstrated 3D resolution enhancement of biological cells using ODT. The authors designed a cycleGAN to learn the optimal transport from those measured 2D projections of a biological sample to the estimated projections along

the inaccessible illumination angles, accordingly, filling up the missing cone in the Fourier space. The reconstruction fidelity was greatly improved, while also taking an order of magnitude less processing time compared to conventional iterative reconstruction methods. This approach that synergistically combines unsupervised learning and physics-based modeling tends to be less prone to overfitting for certain types of samples presented in the training datasets, leading to a strong generalization capability. Without requiring paired training examples, cycleGAN-based approaches also release the requirement of the laborious image registration process and shall be extensively investigated for a wider range of applications in biological studies.

Researchers have further investigated the use of data-driven methods in situations where a large number of training images are unavailable. The latest study reported a self-supervised learning framework termed GedankenNet to eliminate the requirement of experimental training image pairs[96]. By adopting a physics-consistency loss and randomly generated artificial training images with no resemblance to real-world samples, Huang et al. demonstrated that self-supervised learning models could yield superior reconstruction quality and generalization performance than supervised learning models when tested on various unseen biological samples. Another emerging deep learning modality, deep image prior (DIP)[97], performs QPI reconstruction by iteratively optimizing an untrained deep neural network for a given input image, which completely gets rid of the preparation of a training dataset. However, the absence of a dataset also removed the generalization capability of DIP, that is, the iterative optimization process needs to be repeated for every input image, which might take minutes to hours to compute. Albeit this limitation, researchers have demonstrated the success of applying DIP methods to perform QPI reconstruction. Wang et al.[98] utilized DIP combined with Fresnel propagation to achieve phase imaging using a single hologram. Zhou and Horstmeyer[99] used DIP to improve the 3D image quality of stacked microbeads and starfish embryos in diffraction tomography (Fig. 3d). The reconstructions reported in both works outperformed those using conventional iterative methods. The DIP-based method might find its utility in situations where only a single-shot image is available, and the application is not time sensitive.

Another often-practiced method to address the lack of training data is transfer learning, where only a small task-specific dataset is needed to fine-tune a large network that has already been trained by a massive, general-purposed image dataset. Some efforts have been made to facilitate fast transfer learning to new data distributions[100], so that a trained deep neural network on a limited training dataset can be conveniently adapted for QPI reconstruction on input images from unseen subjects and sample types.

Besides exploring the AI-augmented phase recovery methods, researchers have also demonstrated using AI to improve the image quality obtained using traditional QPI systems, such as AI-based noise/aberration reduction and super-resolution. Different neural network architectures have been explored to remove aberration, speckles and coherent noise in QPI images[101–103]. In addition to denoising, neural networks have been shown to be effective and robust for QPI reconstruction at low photon counts, where thermal noise becomes dominant[104,105]. Besides the works that are based on supervised methods, the cycleGAN framework has also been adopted when access to a large training dataset is restricted. For example, to overcome the difficulty in acquiring high-quality noisy and noiseless hologram training pairs, Choi et al.[106] reported a cycleGAN-based tomogram denoising framework that was trained using unpaired clean and noisy RI tomograms. To further enhance the generalization of deep denoising networks, Wu et al.[107] merged the physical forward model of the intensity diffraction tomography with a CNN-based image prior, which outperformed other popular image priors. Other than noise/aberration cancellation, AI also enables super-resolution[108] of the QPI images. Liu et al.[109] presented a U-Net-based super-resolution method suitable for enhancing the performance of various coherent imaging systems (Fig. 3e). In addition, unsupervised learning[110] and DIP-based methods[97] were developed for image super-resolution for natural images.

Segmentation

Segmentation of QPI data can be effectively achieved using AI, providing a starting point for the biomedical application of QPI methods. To create accurate segmentation masks for cellular and subcellular components, U-Net and its variants have been widely used[111]. These approaches typically treat segmentation as pixel-wise classification and train CNNs (or linear classifiers) to predict class probabilities for each pixel. Recent applications have involved the segmentation of diverse cellular structures, such as nuclei, neurites, synapses, membranes and lipid droplets.

As extensively demonstrated in computer vision tasks[112], it has been shown for QPI data that the AI algorithms can generate segmentation masks in a more accurate and faster manner compared to conventional approaches, including manual segmentation[113], ImageJ[28], thresholding and watershed[114] algorithms, which often require manual image processing before the segmentation, thus reducing the efficiency of processing. As one of the pioneering works, Nguyen et al.[115] used the random forest algorithm for the automatic segmentation of prostate cancer tissue images collected using SLIM. Based on the obtained segmentation masks, they subsequently extracted morphological features of Gleason's pattern score, enabling an automatic grading for prostate cancers. Later, using similar QPI data, a U-Net-based model was trained to generate the segmentation masks of subcellular organelles for biological experiments, including tracking of neurite dynamics (Fig. 4a)[116], to determine real-time inference of dry mass for spheroids[54], and to conduct morphological analysis of sperm cells[117].

Another QPI modality to which deep learning-based segmentations have been applied is diffraction tomography. U-Net-inspired networks were trained to take each z plane of cell nuclei of RI tomograms for tracking the morphological dynamics of breast cancer cells[118]. Similarly, Lee et al.[55] proposed an automatic and quantitative spatiotemporal analysis framework for the 3D morphological and biochemical study of immunological cells implementing the U-Net-based segmentation algorithm (Fig. 4b). Unlike the aforementioned deep learning that used 2D U-Net for each z slice, the 3D U-Net-based model, optimized using the neural architecture search, was proposed to perform segmentations for subcellular compartments within a single cell (Fig. 4c)[119]. Here, the complete tomographic information of the specimen was considered in the 3D segmentation network, which would enable accurate subsequent morphological analysis. In addition to the deep learning-based approach, a robust ad hoc clustering algorithm is used for automatic 3D cell nuclei segmentation[120]. We envision this framework would be powerful, particularly when QPI modalities with high-speed sample scanners or microfluidics, which can produce large-scale datasets, are combined[121,122].

Classification

The accurate classification or identification of cell/pathogen types is of great importance in a wide range of life science and biomedical applications, such as clinical disease diagnoses, evaluation of cellular processes, drug discovery screening assays, and microbiome studies[29,30,123–143]. Traditional methods for classifying the cell/pathogen types are based on visual recognition performed by trained experts to distinguish the cells/pathogens, some of which are aided by chemical staining or proliferation. Adopting QPI techniques in classification problems provides a label-free framework with a simplified sample preparation procedure. Introducing AI in such QPI frameworks further increases the system throughput, improves classification accuracy, and makes the system more accessible for nonexperts. More importantly, AI classifiers trained in the supervised learning scheme can usually achieve superhuman classification accuracy. Based on all these strengths, QPI

https://doi.org/10.1038/s41592-023-02041-4

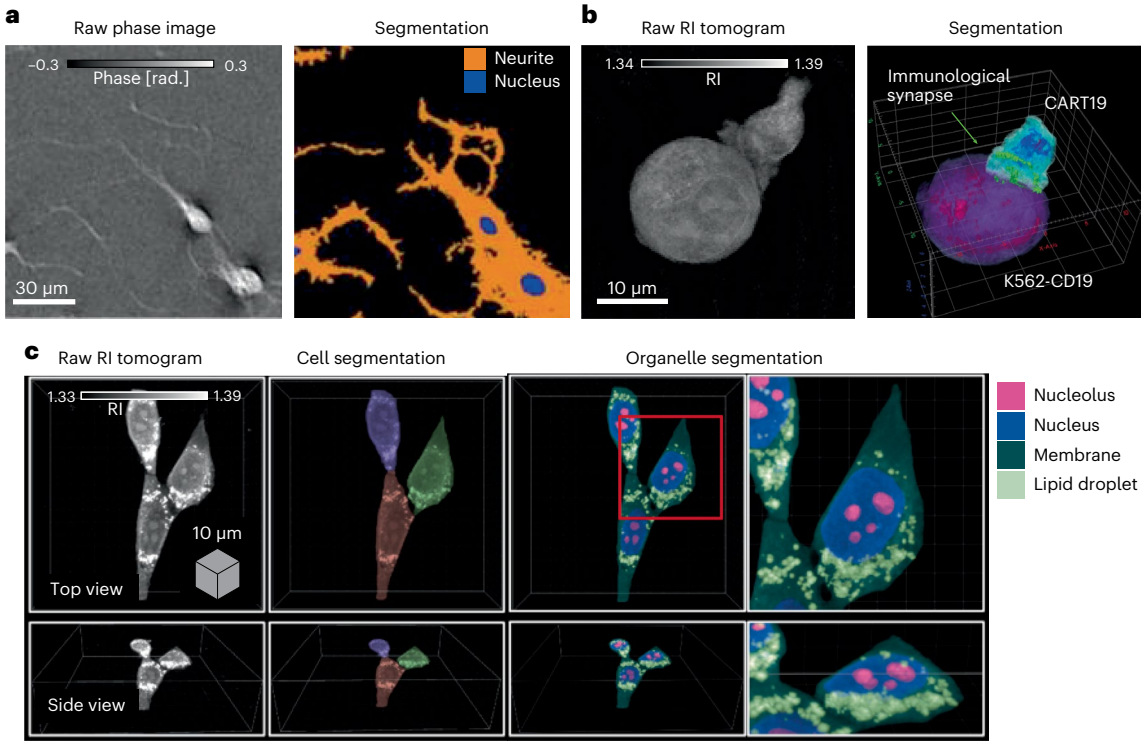

Fig. 4 | Using deep learning for organelle segmentation in QPI images of biological cells. a, Segmentation of neurite and nucleus in the phase images of hippocampal neurons using U-Net-based deep learning[116]. **b**, 3D segmentation of CD19-specific CAR-engineered T (CART19) cells, CD19-positive K561 (K562-CD19) cancer cells and the immunological synapse between the cells in the 3D RI tomogram using U-Net-based deep learning[55]. **c**, 3D segmentation of various subcellular organelles in the 3D RI tomogram of NIH3T3 cells using a 3D U-Net-based algorithm[119].

with AI has been applied to a wide range of classification problems in life science and biomedical research, including the classification of different cancer cells, immune cells, sperm cells, cancer tissues and bacterial species.

Different from the segmentation problem, the output of a classifier is usually a single number representing the class of the input image/video. When the dataset of the input–label pairs is available, a classifier can be trained under the supervised learning framework. Along this direction, researchers have shown that traditional machine learning-based classification methods using QPI may achieve acceptable accuracy in many applications[125–127,129,132–134,139,140,143]. For example, Park et al.[132] demonstrated that the *k*-nearest-neighbor (KNN) algorithm can be used to detect the therapeutic effects of nano-drug delivery (Fig. 5a). Pirone et al. applied the random subspace method to the linear discriminant analysis to identify drug-resistant cancer cells from both 2D phase maps and 3D RI tomograms[143]. Lam et al. and Belashov et al. exploited the support vector machine (SVM) with QPI to quantify epithelial and mesenchymal qualities of cancer cells, predict different cancer cell lines[134] (Fig. 5b) and monitor the photoinduced necrosis in HeLa cells[133]. Also, SVM showed its potential for classifying sperm cells appropriate for in vitro fertilization[144] and classifying cancer cells and normal cells[145]. Other than KNN and SVM, the random forest-based algorithms were implemented by Paidi et al.[140] to coarsely detect different stages of leukemia cells.

Deep learning-based methods were introduced for higher accuracy requirements and more challenging scenarios[29,123,124,128,130,131,135–138,141,142,146,147]. Compared with the hypothesis-driven handcrafted feature extractors in traditional machine learning methods, deep neural networks automatically extract the hidden class-specific features directly from the raw image inputs by learning from the training examples, which often improves the classification accuracy. For example, O'Connor et al. achieved a classification accuracy of 81.52% using a deep learning-based QPI method to distinguish healthy red blood cells and sickle cell disease cells, compared to the 72.93% accuracy obtained by a random forest-based classifier[137]. More complicated cell-type classification and cell status differentiation problems were also studied using deep learning-based QPI approaches including cancer cells[148,149] or sperm cells. For instance, live sperm cells can be classified depending on their status, including normal, DNA fragmentation[150] and stress-affected status (Fig. 5c)[138]. Shu et al. reported an AI-enabled reagent-free imaging hematology analyzer modality that could accurately classify monocytes, granulocytes, lymphocytes and subpopulations of lymphocytes like B and T lymphocytes, $CD4^+$ and $CD8^+$ T cells based on quantitative phase images (Fig. 5d)[142]. Moreover, Zhang et al. obtained 97% accuracy in the classification of benign versus cancer tissue regions with the combination of SLIM and CNNs (Fig. 5e)[146].

The flexibility of the input data format offers the unique capability of the network-based method to process input data with higher dimensionality, such as 3D RI maps, time-lapsed and multispectral images, which often results in very high classification accuracies. For example, by combining 3D RI imaging and deep learning, Park's group obtained >99% accuracy in screening four types of hematological disorders[128], >95% accuracy in classifying human naïve, memory and senescent cells[135], 99.9% accuracy in distinguishing 19 species of bacteria[30] (Fig. 5f), >99% accuracy in the binary classification of myeloid and lymphoid cells and >96% accuracy in differentiating B and T lymphocytes, monocyte and myeloid cells[29]. Wang et al. combined time-lapsed images with a pseudo-3D network and presented an automatic coliform bacteria detection system that could detect growing colonies (that is, colony-forming units) and classify them into correct species within 12 h, shortening the US Environmental Protection Agency (EPA)-approved method by more than 12 h[147]. Similarly, by merging deep learning with time-lapse holographic imaging, Liu et al. developed a stain-free, rapid

https://doi.org/10.1038/s41592-023-02041-4

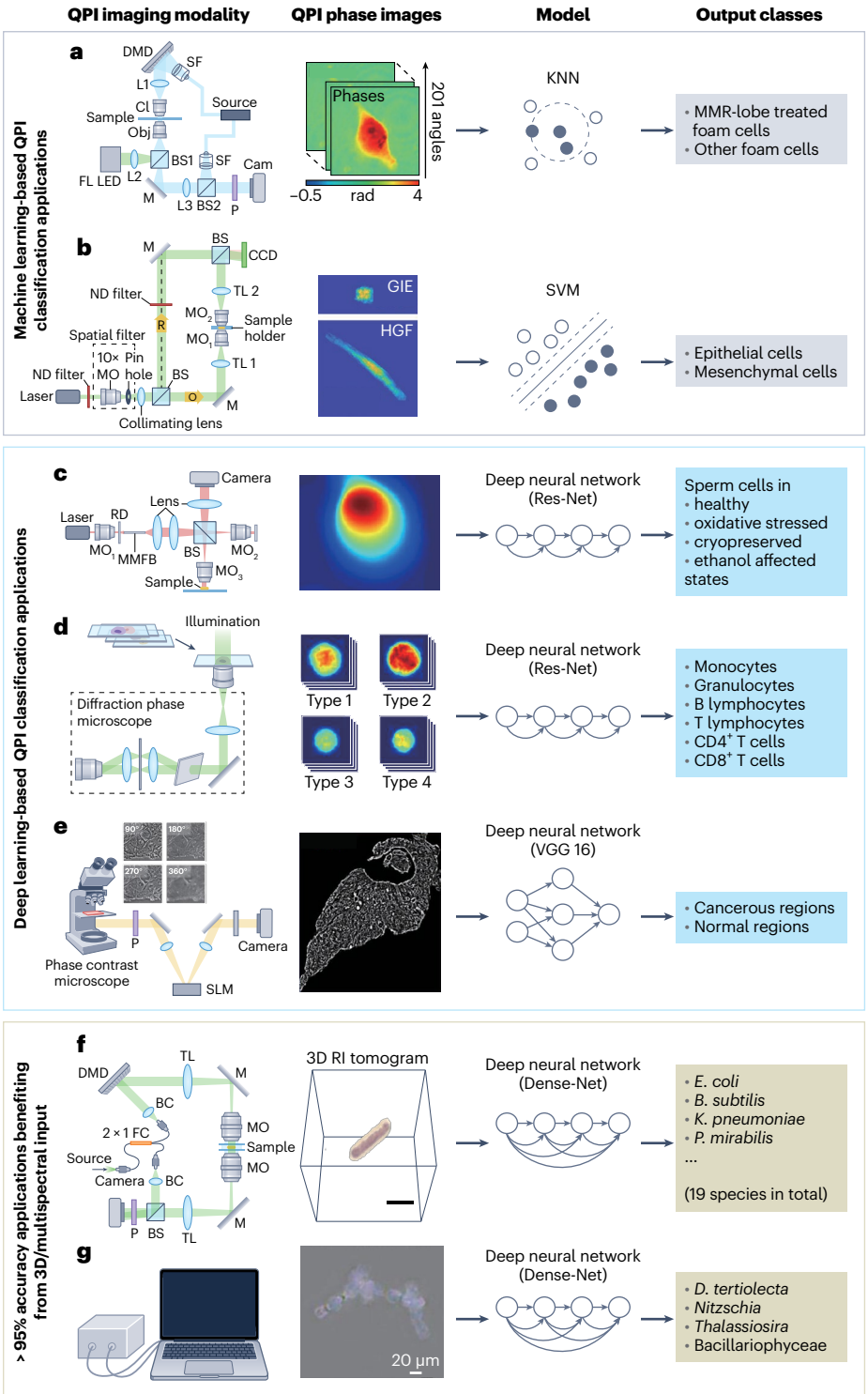

Fig. 5 | Diverse classification applications in life science using QPI and AI. Machine learning-based QPI classification: **a**, Differentiating nano-drug treated foam cells and other foam cells using KNN. Adapted with permission from ref. 132, © 2020 American Chemical Society. **b**, Identifying epithelial and mesenchymal cancer cells using SVM. Adapted from ref. 134, CC BY 4.0. Neural network-based QPI classification: **c**, Classification of normal and stress-affected sperm cells using digital holographic microscopy and ResNet. Adapted from ref. 138, CC BY 4.0. **d**, Leukocytes differentiation achieved using diffraction phase microscopy and ResNet. Adapted from ref. 142, CC BY 4.0. **e**, Classification of cancer and benign tissue regions using VGG16 and SLIM. Adapted from ref. 146, CC BY 4.0. High-accuracy deep learning-based classification applications benefited from 3D/multispectral input: **f**, 99.9% accuracy of identifying 19 bacteria species using ODT and DenseNet. Adapted from ref. 30, CC BY 4.0. **g**, >95% accuracy at distinguishing 4 microalgae cells using multispectral in-line holography and DenseNet. Adapted with permission from ref. 141, © 2021 American Chemical Society.

https://doi.org/10.1038/s41592-023-02041-4

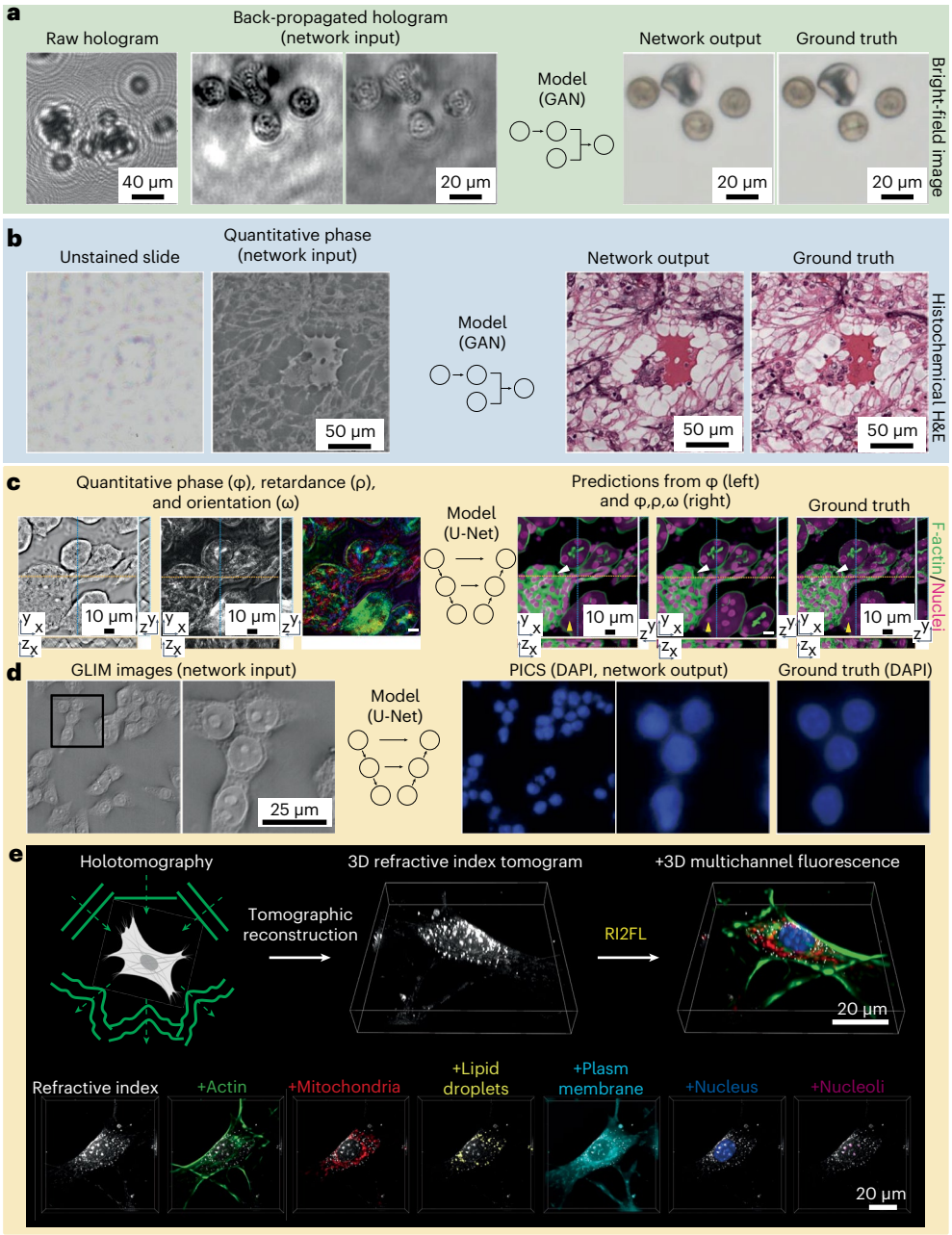

Fig. 6 | AI-enabled image translation from QPI images to other imaging modalities for various biological systems. a, AI translating volumetric QPI images to bright-field color images[83]. **b**, Virtual histochemical (hematoxylin and eosin, H&E) staining of a label-free tissue section[152]. **c**, AI predicting fluorescence labels from quantitative phase, retardance and orientation[156]. **d**, AI virtually staining nucleus and cell membrane[54]. **e**, Multiplexed virtual fluorescence staining using RI and AI[57].

and quantitative viral plaque assay technique that can automatically detect and count >90% plaque-forming units of vesicular stomatitis virus without any false positive within 20 h, saving >24 h and eliminating the staining process compared with traditional plaque assay[151]. Moreover, with the multispectral holographic imaging system and deep learning, Isil et al. achieved >95% accuracy to distinguish four types of microalgae (Fig. 5g)[141].

Cross-modality image-to-image translation

QPI's capability of quantitatively measuring the RI distribution of any label-free, optically transparent object makes it a suitable tool for examining biological samples. However, the direct representation of the RI mapping differs from the conventional imaging methods used in life science studies. AI-enabled image translation from quantitative RI maps into commonly practiced imaging modalities can bridge the gap and provide a transformative way to understand and interpret QPI images. Indeed, deep learning methods to transform QPI images to other modalities, such as bright-field and fluorescence microscopy images, are rapidly emerging. Recent applications include transforming label-free QPI images to multiplexed fluorescence stains capable of detecting cellular structures, including mitochondria and actin, as well as histological stains, such as hematoxylin and eosin or immunohistochemical stains. In contrast to segmentation tasks that identify different regions within an image, based on pixel-level classification, image translation is a generative process that involves transforming an input image to a new image in a different domain or style,

while preserving its semantic content. Note that the image-to-image translation may also facilitate and empower downstream analyses such as image segmentation and classification.

The bright-field microscopic imaging of biological samples with strong absorbance in the visible light band, such as molds and pollens, provides natural contrast for an expert's interpretation. QPI images for these objects, however, are less intuitive. To mitigate this, Wu et al. demonstrated a 'bright-field holography' method, in which a deep neural network was trained to endow the volumetric quantitative phase images with an artifact-free bright-field microscopy contrast (Fig. 6a)[83]. It is different from a QPI reconstruction work in the sense that, it not only retrieves phase information from a single intensity measurement but also colors the samples with natural bright-field contrast. Because only one hologram is used to generate the volumetric bright-field images, the reported high-throughput method can be especially useful for imaging live 3D biological samples with minimal phototoxicity and thermal damage.

Some biological samples, such as tissue sections or cells, typically have very weak absorption at visible wavelengths. The interpretation of these biological specimens under bright-field microscopy is often aided by chromatic staining. A specific example is the inspection of histologically stained tissue sections, which plays an important role in the diagnosis of diverse human diseases. In this regard, transforming phase images of the tissue sections to the equivalent bright-field images after staining, that is, virtual staining, has been reported for a wide range of applications. Rivenson et al. presented a demonstration of a deep learning-enabled PhaseStain approach, which transforms QPI images of various label-free tissue sections into bright-field images that are equivalent to the histochemically stained ones (Fig. 6b)[152]. By generating virtually stained images of the tissue slides, the presented data-driven approach achieved unprecedented simplification in sample treatment processes and reduction in time, labor and cost. The reported deep learning-based virtual staining approach, which was performed using lens-free in-line holography, can also be widely adapted to other QPI techniques. In another research, Wang et al. reported an unsupervised virtual bright-field and fluorescence staining method for Fourier ptychography[153]. A cycleGAN was trained to restore the color information of the immunohistochemically stained or fluorescence-labeled samples from their monochromatic FPM images (intensity or phase).

In addition to tissue examination, the analysis of individual biological cells can also benefit from the combination of QPI and AI. Nygate et al. demonstrated the virtual staining of sperm cells using holographic imaging and deep learning[154]. The off-axis holographic images of the unstained sperm cells were fed into a trained GAN model to predict the bright-field images of the sperms as if they had been chemically stained. The virtual staining of the sperm cells can lead to the automatic fertility stratification[155], which might provide clinicians with a more natural and straightforward way for the morphological analysis of the sperms.

Besides bright-field microscopy, fluorescence microscopy has also been used as an essential imaging tool that provides molecular-specific contrast for the study of biological systems. However, the utility of fluorescence microscopy is limited by certain drawbacks such as photobleaching, phototoxicity and spectral overlaps, which are difficult to overcome in typical implementations. Recent advances in combining QPI and AI-enabled cross-modality inference have posted new solutions to these challenges. Guo et al. reported a new approach named quantitative label-free imaging with phase and polarization (QLIPP) for simultaneous measurement of density, anisotropy and orientation of structures in unlabeled live cells and tissue slices[156]. Multichannel 2.5D U-Nets were trained to predict the 3D fluorescence distribution from label-free QLIPP images (quantitative phase, retardance and orientation) or quantitative phase only. A robust and accurate prediction of fluorescence labels of both anisotropic and isotropic structures (F-actin and nuclei) in mouse kidneys was demonstrated (Fig. 6c).

Compared to fluorescence imaging, the nondestructive nature of QPI makes it advantageous in live cell inspection. Kandel et al. presented phase imaging with computational specificity (PICS), which generates the subcellular specificity that conventionally requires molecularly specific labeling, for unlabeled live cells using the combination of QPI and AI[54]. A trained network inference model was built into a real-time acquisition software to predict the DAPI (nucleus) and DiI (cell membrane) fluorophores from label-free quantitative phase images (Fig. 6d). Then, the inferred fluorescence maps were applied back to the QPI data for the real-time measurement of the dry mass of nuclei and cytoplasm. Due to the absence of chemical toxicity and photobleaching, PICS can perform dynamic imaging of live cells over extended periods without cell viability concerns, which offers a quantitative technique for long-term monitoring of individual cellular components in biological applications. Furthermore, the deep learning-based multiplexed virtual staining approach provides a fast, affordable and simplified way to analyze biological samples, by mapping the QPI data to fluorescent stains. Jo et al. demonstrated a data-driven technology RI2FL for label-free multiplexed microtomography of endogenous subcellular structures using deep learning[57]. The presented RI2FL is a scalable framework that can infer multiple subcellular fluorescent stains such as mitochondria, actin and nuclei from the 3D RI tomograms (Fig. 6e). As RI is an absolute and unbiased intrinsic quantity of the biological materials, the approach based on a full 3D modeling of RI can be generalized to a broad range of new samples without retraining. The performance, reliability and scalability of this technology were extensively characterized, and its applications within high-throughput single-cell profiling were demonstrated.

Outlook

AI has been fueling biological studies using QPI, enabling time-efficient reconstruction, accurate segmentation and classification, and cross-modality image transformations. Along with the advancements, concerns were raised about potential hallucinations created by a neural network reconstructing a QPI image, and doubts grew regarding the validity of an image translated from a QPI using AI. The successful demonstrations so far have pronounced the validity of AI. Rigorous analysis has been conducted to address the concerns by quantifying the uncertainty of neural networks[157,158]. As we venture further, it is vital to uphold stringent standards in model training and deployment to maintain the credibility of AI in QPI studies. This includes the critical steps of ensuring that models are trained and deployed on matching datasets, vigilantly avoiding overfitting and, whenever feasible or periodically, benchmarking output images against ground truth for performance validation. Along a similar direction, it is desirable to establish a quantitative benchmark to analyze the uncertainty of using AI in QPI. Based on this benchmark, when the uncertainty generated by AI reaches a similar or lower level compared to the inter-instrument and inter-algorithm variabilities of the conventional methods, the AI-aided QPI can be widely adapted to routine applications. Further efforts shall be made in two directions: to utilize AI to solve QPI problems that are impossible to achieve using conventional methods, and to codesign a QPI system with the help of AI. Firstly, AI has the potential to boost in vivo QPI for biological samples, which requires imaging through scattering mediums like 3D live tissue. For example, coherent imaging through scattering media (for example, ground glass, multimode fibers) has been successfully realized by training CNNs that recognize and reconstruct objects from speckle patterns[159,160]. Later, a trained CNN generalizable to different medium perturbations was demonstrated to successfully predict objects through unseen diffusers in the training stage[161]. Recently, RNNs, which have been commonly utilized for processing sequential data, were also explored for 2D and 3D QPI[84], also demonstrating their capability of imaging through strongly scattering media[162,163]. These works highlight the power of AI in reconstructing the in-depth features behind the scattering media, which is fundamental to

potential future explorations of applying AI and QPI to in vivo biological studies that are currently intractable.

Secondly, building a QPI system with AI, or codesigning an imaging system with the help of AI, can be another exciting possibility. Recently, data-driven methods have been successfully used in optimizing illumination patterns in Fourier ptychography[164–166]. Kellman et al.[164] proposed a data-driven design framework that learns efficient LED source patterns while simultaneously relaxing required measurement constraints. More recently, the combination of AI and diffractive optics enabled all-optical quantitative phase-to-amplitude mapping without the need for a computer[167]: Mengu et al.[167] presented a diffractive neural network[168–170], which computes using the light-matter interaction on AI-designed successive diffractive layers and free space propagation in between, to directly convert the phase information of an input object to the intensity distribution at the output plane, at the speed of light. The same diffractive neural network platform was also used to demonstrate the computer-free, all-optical reconstruction of holograms[171]. The combination of AI-enabled QPI and flow cytometry system may potentially expand the applicability by sorting different cell types in a label-free manner[172,173]. These AI-designed QPI systems can potentially replace traditional complicated QPI setups and will provide new research tools for developing real-time holographic imaging and QPI systems that energize different applications.

In conclusion, a synergistic combination of AI and QPI has recently gained tremendous success in biological imaging. AI has already proven invaluable for both enhancing the performance of QPI and providing a way to efficiently interpret the resulting images. These data-driven approaches also have promising potential to reduce the time and cost in diverse aspects of QPI, leading to the broadening utility of QPI in life sciences.

References

1. Milestones in light microscopy. *Nat. Cell Biol.* **11**, 1165 (2009).
2. Lee, K. et al. Quantitative phase imaging techniques for the study of cell pathophysiology: from principles to applications. *Sensors* **13**, 4170–4191 (2013).
3. Kim, K. et al. Optical diffraction tomography techniques for the study of cell pathophysiology. *J. Biomed. Photonics Eng.* **2**, 020201 (2016).
4. Popescu, G. Quantitative phase imaging of cells and tissues (McGraw-Hill Education, 2011).
5. Park, Y., Depeursinge, C. & Popescu, G. Quantitative phase imaging in biomedicine. *Nat. Photonics* **12**, 578–589 (2018).
6. LeCun, Y., Bengio, Y. & Hinton, G. Deep learning. *Nature* **521**, 436–444 (2015).
7. Zernike, F. How I discovered phase contrast. *Science* **121**, 345–349 (1955).
8. Nomarski, G. Microinterféromètre différentiel à ondes polarisées. *J. Phys. Rad.* **16**, 9S–13S (1955).
9. Marquet, P. et al. Digital holographic microscopy: a noninvasive contrast imaging technique allowing quantitative visualization of living cells with subwavelength axial accuracy. *Opt. Lett.* **30**, 468–470 (2005).
10. Popescu, G., Ikeda, T., Dasari, R. R. & Feld, M. S. Diffraction phase microscopy for quantifying cell structure and dynamics. *Opt. Lett.* **31**, 775–777 (2006).
11. Ikeda, T., Popescu, G., Dasari, R. R. & Feld, M. S. Hilbert phase microscopy for investigating fast dynamics in transparent systems. *Opt. Lett.* **30**, 1165–1167 (2005).
12. Zuo, C. et al. Transport of intensity equation: a tutorial. *Opt. Lasers Eng.* **135**, 106187 (2020).
13. Soto, J. M., Rodrigo, J. A. & Alieva, T. Optical diffraction tomography with fully and partially coherent illumination in high numerical aperture label-free microscopy [Invited]. *Appl. Opt.* **57**, A205–A214 (2018).
14. Baek, Y. & Park, Y. Intensity-based holographic imaging via space-domain Kramers–Kronig relations. *Nat. Photonics* **15**, 354–360 (2021).
15. Tian, L. & Waller, L. Quantitative differential phase contrast imaging in an LED array microscope. *Opt. Express* **23**, 11394–11403 (2015).
16. Zheng, G., Horstmeyer, R. & Yang, C. Wide-field, high-resolution Fourier ptychographic microscopy. *Nat. Photonics* **7**, 739–745 (2013).
17. Abbe, E. Beiträge zur Theorie des Mikroskops und der mikroskopischen Wahrnehmung. *Arch. für. Mikroskop. Anat.* **9**, 413–468 (1873).
18. Skylaki, S., Hilsenbeck, O. & Schroeder, T. Challenges in long-term imaging and quantification of single-cell dynamics. *Nat. Biotechnol.* **34**, 1137–1144 (2016).
19. Magidson, V. & Khodjakov, A. Circumventing photodamage in live-cell microscopy. *Methods Cell. Biol.* **114**, 545–560 (2013).
20. Huisken, J., Swoger, J., Del Bene, F., Wittbrodt, J. & Stelzer, E. H. Optical sectioning deep inside live embryos by selective plane illumination microscopy. *Science* **305**, 1007–1009 (2004).
21. Weber, M., Mickoleit, M. & Huisken, J. Light sheet microscopy. *Methods Cell. Biol.* **123**, 193–215 (2014).
22. Denk, W., Strickler, J. H. & Webb, W. W. Two-photon laser scanning fluorescence microscopy. *Science* **248**, 73–76 (1990).
23. Helmchen, F. & Denk, W. Deep tissue two-photon microscopy. *Nat. Methods* **2**, 932–940 (2005).
24. Axelrod, D., Burghardt, T. P. & Thompson, N. L. Total internal reflection fluorescence. *Annu. Rev. Biophys. Bioeng.* **13**, 247–268 (1984).
25. Axelrod, D. Total internal reflection fluorescence microscopy in cell biology. *Traffic* **2**, 764–774 (2001).
26. Subedi, N. R. et al. Integrative quantitative-phase and airy light-sheet imaging. *Sci. Rep.* **10**, 20150 (2020).
27. Icha, J., Weber, M., Waters, J. C. & Norden, C. Phototoxicity in live fluorescence microscopy, and how to avoid it. *BioEssays* **39**, 1700003 (2017).
28. Lee, A. J. et al. Label-free monitoring of 3D cortical neuronal growth in vitro using optical diffraction tomography. *Biomed. Opt. Express* **12**, 6928–6939 (2021).
29. Ryu, D. et al. Label-free white blood cell classification using refractive index tomography and deep learning. *BME Front.* **2021**, 9893804 (2021).
30. Kim, G. et al. Rapid species identification of pathogenic bacteria from a minute quantity exploiting three-dimensional quantitative phase imaging and artificial neural network. *Light Sci. Appl.* **11**, 190 (2022).
Rapid label-free classification of bacterial species using QPI and deep learning. The framework utilizes a single 3D QPI image to accurately classify different bacterial species, without the need for labeling.
31. Carrigan, S. D., Scott, G. & Tabrizian, M. Toward resolving the challenges of sepsis diagnosis. *Clin. Chem.* **50**, 1301–1314 (2004).
32. Barer, R. Interference microscopy and mass determination. *Nature* **169**, 366–367 (1952).
33. Davies, H. & Wilkins, M. Interference microscopy and mass determination. *Nature* **169**, 541–541 (1952).
34. Gabor, D. A new microscopic principle. *Nature* **161**, 777–778 (1948).
A demonstration of holographic microscopy.
35. Bruning, J. H. et al. Digital wavefront measuring interferometer for testing optical surfaces and lenses. *Appl. Opt.* **13**, 2693–2703 (1974).
36. Yamaguchi, I. & Zhang, T. Phase-shifting digital holography. *Opt. Lett.* **22**, 1268–1270 (1997).
37. Yamaguchi, I., Kato, J.-i, Ohta, S. & Mizuno, J. Image formation in phase-shifting digital holography and applications to microscopy. *Appl. Opt.* **40**, 6177–6186 (2001).

38. Takeda, M., Ina, H. & Kobayashi, S. Fourier-transform method of fringe-pattern analysis for computer-based topography and interferometry. *J. Opt. Soc. Am* **72**, 156–160 (1982).
39. Leith, E. N. & Upatnieks, J. Reconstructed wavefronts and communication theory. *J. Opt. Soc. Am.* **52**, 1123–1130 (1962).
40. Wang, Z. et al. Spatial light interference microscopy (SLIM). *Opt. Express* **19**, 1016–1026 (2011).
41. Bhaduri, B., Pham, H., Mir, M. & Popescu, G. Diffraction phase microscopy with white light. *Opt. Lett.* **37**, 1094–1096 (2012).
42. Zheng, G., Shen, C., Jiang, S., Song, P. & Yang, C. Concept, implementations and applications of Fourier ptychography. *Nat. Rev. Phys.* **3**, 207–223 (2021).
43. Oh, C., Isikman, S. O., Khademhosseinieh, B. & Ozcan, A. On-chip differential interference contrast microscopy using lensless digital holography. *Opt. Express* **18**, 4717–4726 (2010).
44. Bon, P., Maucort, G., Wattellier, B. & Monneret, S. Quadriwave lateral shearing interferometry for quantitative phase microscopy of living cells. *Opt. Express* **17**, 13080–13094 (2009).
45. Nguyen, T. H., Kandel, M. E., Rubessa, M., Wheeler, M. B. & Popescu, G. Gradient light interference microscopy for 3D imaging of unlabeled specimens. *Nat. Commun.* **8**, 210 (2017).
46. Seo, S., Su, T. -W., Tseng, D. K., Erlinger, A. & Ozcan, A. Lensfree holographic imaging for on-chip cytometry and diagnostics. *Lab Chip* **9**, 777–787 (2009).
47. Greenbaum, A. et al. Imaging without lenses: achievements and remaining challenges of wide-field on-chip microscopy. *Nat. Methods* **9**, 889–895 (2012).
48. Su, T. -W., Xue, L. & Ozcan, A. High-throughput lensfree 3D tracking of human sperms reveals rare statistics of helical trajectories. *Proc. Natl Acad. Sci. USA* **109**, 16018–16022 (2012).
49. Zuo, C., Sun, J., Zhang, J., Hu, Y. & Chen, Q. Lensless phase microscopy and diffraction tomography with multi-angle and multi-wavelength illuminations using a LED matrix. *Opt. Express* **23**, 14314–14328 (2015).
50. Teague, M. R. Irradiance moments: their propagation and use for unique retrieval of phase. *J. Opt. Soc. Am.* **72**, 1199–1209 (1982).
51. Teague, M. R. Deterministic phase retrieval: a Green's function solution. *J. Opt. Soc. Am.* **73**, 1434–1441 (1983).
52. Tian, L. & Waller, L. 3D intensity and phase imaging from light field measurements in an LED array microscope. *Optica* **2**, 104–111 (2015).
53. Chen, M., Tian, L. & Waller, L. 3D differential phase contrast microscopy. *Biomed. Opt. Express* **7**, 3940–3950 (2016).
54. Kandel, M. E. et al. Phase imaging with computational specificity (PICS) for measuring dry mass changes in sub-cellular compartments. *Nat. Commun.* **11**, 6256 (2020).
55. Lee, M. et al. Deep-learning-based three-dimensional label-free tracking and analysis of immunological synapses of CAR-T cells. *Elife* **9**, e49023 (2020).
Study on dynamics of immunological synapses of CAR-T cells through automatic segmentation of the synapses from label-free QPI images using deep learning.
56. Goswami, N. et al. Label-free SARS-CoV-2 detection and classification using phase imaging with computational specificity. *Light Sci. Appl.* **10**, 176 (2021).
57. Jo, Y. et al. Label-free multiplexed microtomography of endogenous subcellular dynamics using generalizable deep learning. *Nat. Cell Biol.* **23**, 1329–1337 (2021).
Study on highly multiplexed virtual staining of label-free QPI images using deep learning. The framework transforms a single label-free cellular QPI image into multiple fluorescence-labeled images, providing multiple subcellular specificities simultaneously.
58. Wolf, E. Three-dimensional structure determination of semi-transparent objects from holographic data. *Opt. Commun.* **1**, 153–156 (1969).
59. Isikman, S. O., Bishara, W. & Ozcan, A. Partially coherent lensfree tomographic microscopy. *Appl. Opt.* **50**, H253–H264 (2011).
60. Isikman, S. O. et al. Lens-free optical tomographic microscope with a large imaging volume on a chip. *Proc. Natl Acad. Sci. USA* **108**, 7296–7301 (2011).
61. Hugonnet, H., Lee, M. & Park, Y. Optimizing illumination in three-dimensional deconvolution microscopy for accurate refractive index tomography. *Opt. Express* **29**, 6293–6301 (2021).
62. Hugonnet, H., Lee, M. J. & Park, Y. K. Quantitative phase and refractive index imaging of 3D objects via optical transfer function reshaping. *Opt. Express* **30**, 13802–13809 (2022).
63. Kamilov, U. S. et al. Learning approach to optical tomography. *Optica* **2**, 517–522 (2015).
64. Lim, J., Ayoub, A. B., Antoine, E. E. & Psaltis, D. High-fidelity optical diffraction tomography of multiple scattering samples. *Light Sci. Appl.* **8**, 82 (2019).
65. Fan, S., Smith-Dryden, S., Li, G. & Saleh, B. Reconstructing complex refractive-index of multiply-scattering media by use of iterative optical diffraction tomography. *Opt. Express* **28**, 6846–6858 (2020).
66. Lee, M., Hugonnet, H. & Park, Y. Inverse problem solver for multiple light scattering using modified Born series. *Optica* **9**, 177–182 (2022).
67. Merola, F. et al. Tomographic flow cytometry by digital holography. *Light Sci. Appl.* **6**, e16241 (2017).
68. Lee, M. et al. High-resolution assessment of multidimensional cellular mechanics using label-free refractive-index traction force microscopy. Preprint at *bioRxiv* https://doi.org/10.1101/2023.02.15.528626 (2023).
69. Vasdekis, A. E. et al. Eliciting the impacts of cellular noise on metabolic trade-offs by quantitative mass imaging. *Nat. Commun.* **10**, 848 (2019).
70. Kandel, M. E., Teng, K. W., Selvin, P. R. & Popescu, G. Label-free imaging of single microtubule dynamics using spatial light interference microscopy. *ACS Nano* **11**, 647–655 (2017).
71. Lee, C. et al. Label-free three-dimensional observations and quantitative characterisation of on-chip vasculogenesis using optical diffraction tomography. *Lab Chip* **21**, 494–501 (2021).
72. Park, J. et al. Quantification of structural heterogeneity in H&E stained clear cell renal cell carcinoma using refractive index tomography. *Biomed. Opt. Express* **14**, 1071–1081 (2023).
73. Bokemeyer, A. et al. Quantitative phase imaging using digital holographic microscopy reliably assesses morphology and reflects elastic properties of fibrotic intestinal tissue. *Sci. Rep.* **9**, 19388 (2019).
74. Chetlur, S. et al. cudnn: efficient primitives for deep learning. Preprint at https://doi.org/10.48550/arXiv.1410.0759 (2014).
75. Paszke, A. et al. PyTorch: an imperative style, high-performance deep learning library. *Advances in Neural Information Processing Systems* **32**, 8026–8037 (2019).
Introduction of Pytorch, which enabled efficient access to deep learning frameworks, making it one of the most widely used machine learning libraries in the current era.
76. Abadi, M. et al. TensorFlow: a system for large-scale machine learning. *OSDI* **16**, 265–283 (2016).
Introduction of TensorFlow, one of the most extensively utilized machine learning libraries, which has substantially enhanced the usability of machine learning algorithms.
77. Lim, J. et al. Comparative study of iterative reconstruction algorithms for missing cone problems in optical diffraction tomography. *Opt. Express* **23**, 16933–16948 (2015).
78. Petrou, M. M. & Petrou, C. *Image Processing: the Fundamentals* (John Wiley & Sons, 2010).

79. Rivenson, Y., Zhang, Y., Gunaydin, H., Teng, D. & Ozcan, A. Phase recovery and holographic image reconstruction using deep learning in neural networks. *Light Sci. Appl.* **7**, 17141 (2018). **An early study on rapid image reconstruction in holographic imaging using deep learning**.
80. Nguyen, T., Xue, Y., Li, Y., Tian, L. & Nehmetallah, G. Deep learning approach for Fourier ptychography microscopy. *Opt. Express* **26**, 26470–26484 (2018).
81. Barbastathis, G., Ozcan, A. & Situ, G. On the use of deep learning for computational imaging. *Optica* **6**, 921–943 (2019).
82. Wu, Y. et al. Extended depth-of-field in holographic imaging using deep-learning-based autofocusing and phase recovery. *Optica* **5**, 704–710 (2018).
83. Wu, Y. et al. Bright-field holography: cross-modality deep learning enables snapshot 3D imaging with bright-field contrast using a single hologram. *Light Sci. Appl.* **8**, 25 (2019).
84. Huang, L. et al. Holographic image reconstruction with phase recovery and autofocusing using recurrent neural networks. *ACS Photonics* **8**, 1763–1774 (2021).
85. Chen, H., Huang, L., Liu, T. & Ozcan, A. Fourier Imager Network (FIN): a deep neural network for hologram reconstruction with superior external generalization. *Light Sci. Appl.* **11**, 254 (2022).
86. Pirone, D. et al. Speeding up reconstruction of 3D tomograms in holographic flow cytometry via deep learning. *Lab Chip* **22**, 793–804 (2022).
87. Xue, Y., Cheng, S., Li, Y. & Tian, L. Reliable deep-learning-based phase imaging with uncertainty quantification. *Optica* **6**, 618–629 (2019).
88. Dardikman-Yoffe, G. et al. PhUn-Net: ready-to-use neural network for unwrapping quantitative phase images of biological cells. *Biomed. Opt. Express* **11**, 1107–1121 (2020).
89. Ryu, D. et al. DeepRegularizer: rapid resolution enhancement of tomographic imaging using deep learning. *IEEE Trans. Med. Imaging* **40**, 1508–1518 (2021).
90. Lim, J., Ayoub, A. B. & Psaltis, D. Three-dimensional tomography of red blood cells using deep learning. *Adv. Photonics* **2**, 026001 (2020).
91. Zhu, J.-Y., Park, T., Isola, P. & Efros, A. A. Unpaired image-to-image translation using cycle-consistent adversarial networks. In *Proc. IEEE International Conference on Computer Vision* 2223–2232 (IEEE, 2017).
92. Yin, D. et al. Digital holographic reconstruction based on deep learning framework with unpaired data. *IEEE Photonics J.* **12**, 1–12 (2019).
93. Zuo, C., Chen, Q., Qu, W. & Asundi, A. Phase aberration compensation in digital holographic microscopy based on principal component analysis. *Opt. Lett.* **38**, 1724–1726 (2013).
94. Zhang, Y. et al. PhaseGAN: a deep-learning phase-retrieval approach for unpaired datasets. *Opt. Express* **29**, 19593–19604 (2021).
95. Chung, H., Huh, J., Kim, G., Park, Y. K. & Ye, J. C. Missing cone artifact removal in odt using unsupervised deep learning in the projection domain. *IEEE Trans. Comput. Imaging* **7**, 747–758 (2021).
96. Huang, L. et al. Self-supervised learning of hologram reconstruction using physics consistency. *Nat. Mach. Intell.* **5**, 895–907 (2023).
97. Ulyanov, D., Vedaldi, A. & Lempitsky, V. Deep image prior. In *Proc. IEEE Conf. Computer Vision and Pattern Recognition* 9446–9454 (IEEE. 2018).
98. Wang, F. et al. Phase imaging with an untrained neural network. *Light Sci. Appl.* **9**, 77 (2020).
99. Zhou, K. C. & Horstmeyer, R. Diffraction tomography with a deep image prior. *Opt. Express* **28**, 12872–12896 (2020).
100. Huang, L., Yang, X., Liu, T. & Ozcan, A. Few-shot transfer learning for holographic image reconstruction using a recurrent neural network. *APL Photonics* **7**, 070801 (2022).
101. Chang, T. et al. Calibration-free quantitative phase imaging using data-driven aberration modeling. *Opt. Express* **28**, 34835–34847 (2020).
102. Park, D.-Y. & Park, J.-H. Hologram conversion for speckle free reconstruction using light field extraction and deep learning. *Opt. Express* **28**, 5393–5409 (2020).
103. Chen, L., Chen, X., Cui, H., Long, Y. & Wu, J. Image enhancement in lensless inline holographic microscope by inter-modality learning with denoising convolutional neural network. *Opt. Commun.* **484**, 126682 (2021).
104. Goy, A., Arthur, K., Li, S. & Barbastathis, G. Low photon count phase retrieval using deep learning. *Phys. Rev. Lett.* **121**, 243902 (2018).
105. Deng, M., Li, S., Goy, A., Kang, I. & Barbastathis, G. Learning to synthesize: robust phase retrieval at low photon counts. *Light Sci. Appl.* **9**, 36 (2020).
106. Choi, G. et al. Cycle-consistent deep learning approach to coherent noise reduction in optical diffraction tomography. *Opt. Express* **27**, 4927–4943 (2019).
107. Wu, Z. et al. SIMBA: scalable inversion in optical tomography using deep denoising priors. *IEEE J. Sel. Top. Signal Process.* **14**, 1163–1175 (2020).
108. Rivenson, Y. et al. Deep learning microscopy. *Optica* **4**, 1437–1443 (2017).
109. Liu, T. et al. Deep learning-based super-resolution in coherent imaging systems. *Sci. Rep.* **9**, 3926 (2019). **Resolution enhancement of both amplitude and phase images in a holographic imaging system using deep learning**.
110. Yuan, Y. et al. Unsupervised image super-resolution using cycle-in-cycle generative adversarial networks. In *Proc. IEEE Conf. Computer Vision and Pattern Recognition Workshops*, 701–710 (IEEE, 2018).
111. Rizwan, I., Haque, I. & Neubert, J. Deep learning approaches to biomedical image segmentation. *Inform. Med. Unlocked* **18**, 100297 (2020).
112. Minaee, S. et al. Image segmentation using deep learning: a survey. *IEEE Trans. Pattern Anal. Mach. Intell.* **44**, 3523–3542 (2021).
113. Wang, P., Bista, R., Bhargava, R., Brand, R. E. & Liu, Y. Spatial-domain low-coherence quantitative phase microscopy for cancer diagnosis. *Opt. Lett.* **35**, 2840–2842 (2010).
114. Pal, N. R. & Pal, S. K. A review on image segmentation techniques. *Pattern Recognition* **26**, 1277–1294 (1993).
115. Nguyen, T. H. et al. Automatic Gleason grading of prostate cancer using quantitative phase imaging and machine learning. *J. Biomed. Opt.* **22**, 36015 (2017).
116. Kandel, M. E. et al. Multiscale assay of unlabeled neurite dynamics using phase imaging with computational specificity. *ACS Sens.* **6**, 1864–1874 (2021).
117. Kandel, M. E. et al. Reproductive outcomes predicted by phase imaging with computational specificity of spermatozoon ultrastructure. *Proc. Natl Acad. Sci. USA* **117**, 18302–18309 (2020).
118. Lee, J. et al. Deep-learning-based label-free segmentation of cell nuclei in time-lapse refractive index tomograms. *IEEE Access* **7**, 83449–83460 (2019).
119. Choi, J. et al. Label-free three-dimensional analyses of live cells with deep-learning-based segmentation exploiting refractive index distributions. Preprint at *bioRxiv* https://doi.org/10.1101/2021.05.23.445351 (2021).
120. Pirone, D. et al. Stain-free identification of cell nuclei using tomographic phase microscopy in flow cytometry. *Nat. Photonics* **16**, 851–859 (2022).
121. Hugonnet, H. et al. Multiscale label-free volumetric holographic histopathology of thick-tissue slides with subcellular resolution. *Adv. Photonics* **3**, 026004 (2021).

122. Nitta, N. et al. Intelligent image-activated cell sorting. *Cell* **175**, 266–276 (2018).
123. Chen, C. L. et al. Deep learning in label-free cell classification. *Sci. Rep.* **6**, 21471 (2016).
An early study on the utilization of deep learning integrated with QPI for label-free cell type classification.
124. Jo, Y. et al. Holographic deep learning for rapid optical screening of anthrax spores. *Sci. Adv.* **3**, e1700606 (2017).
125. Pavillon, N., Hobro, A. J., Akira, S. & Smith, N. I. Noninvasive detection of macrophage activation with single-cell resolution through machine learning. *Proc. Natl Acad. Sci. USA* **115**, E2676–E2685 (2018).
126. Go, T., Kim, J. H., Byeon, H. & Lee, S. J. Machine learning-based in-line holographic sensing of unstained malaria-infected red blood cells. *J. Biophotonics* **11**, e201800101 (2018).
127. Javidi, B. et al. Sickle cell disease diagnosis based on spatio-temporal cell dynamics analysis using 3D printed shearing digital holographic microscopy. *Opt. Express* **26**, 13614–13627 (2018).
128. Kim, G., Jo, Y., Cho, H., Min, H. S. & Park, Y. Learning-based screening of hematologic disorders using quantitative phase imaging of individual red blood cells. *Biosens. Bioelectron.* **123**, 69–76 (2019).
129. Ozaki, Y. et al. Label-free classification of cells based on supervised machine learning of subcellular structures. *PLoS ONE* **14**, e0211347 (2019).
130. Karandikar, S. H. et al. Reagent-free and rapid assessment of T cell activation state using diffraction phase microscopy and deep learning. *Anal. Chem.* **91**, 3405–3411 (2019).
131. Rubin, M. et al. TOP-GAN: Stain-free cancer cell classification using deep learning with a small training set. *Med. Image Anal.* **57**, 176–185 (2019).
132. Park, S. et al. Label-free tomographic imaging of lipid droplets in foam cells for machine-learning-assisted therapeutic evaluation of targeted nanodrugs. *ACS Nano* **14**, 1856–1865 (2020).
133. Belashov, A. V. et al. In vitro monitoring of photoinduced necrosis in HeLa cells using digital holographic microscopy and machine learning. *J. Opt. Soc. Am. A Opt. Image Sci. Vis.* **37**, 346–352 (2020).
134. Lam, V. et al. Quantitative scoring of epithelial and mesenchymal qualities of cancer cells using machine learning and quantitative phase imaging. *J. Biomed. Opt.* **25**, 1–17 (2020).
135. Ryu, D. et al. Label-free 3D quantitative phase imaging cytometry with deep learning: identifying naive, memory, and senescent T cells. *J. Immunol.* **204**, 86.5 (2020).
136. Singla, N. & Srivastava, V. Deep learning enabled multi-wavelength spatial coherence microscope for the classification of malaria-infected stages with limited labelled data size. *Opt. Laser Technol.* **130**, 106335 (2020).
137. O'Connor, T., Anand, A., Andemariam, B. & Javidi, B. Deep learning-based cell identification and disease diagnosis using spatio-temporal cellular dynamics in compact digital holographic microscopy. *Biomed. Opt. Express* **11**, 4491–4508 (2020).
138. Butola, A. et al. High spatially sensitive quantitative phase imaging assisted with deep neural network for classification of human spermatozoa under stressed condition. *Sci. Rep.* **10**, 13118 (2020).
139. Nissim, N., Dudaie, M., Barnea, I. & Shaked, N. T. Real-time stain-free classification of cancer cells and blood cells using interferometric phase microscopy and machine learning. *Cytom. Part A* **99**, 511–523 (2021).
140. Paidi, S. K. et al. Raman and quantitative phase imaging allow morpho-molecular recognition of malignancy and stages of B-cell acute lymphoblastic leukemia. *Biosens. Bioelectron.* **190**, 113403 (2021).
141. Işıl, C. A. A. et al. Phenotypic analysis of microalgae populations using label-free imaging flow cytometry and deep learning. *ACS Photonics* **8**, 1232–1242 (2021).
High-throughput classification of microalgae species using QPI and deep learning.
142. Shu, X. et al. Artificial-intelligence-enabled reagent-free imaging hematology analyzer. *Adv. Intell. Syst.* **3**, 2000277 (2021).
Rapid label-free classification of white blood cells using QPI and deep learning techniques. The framework achieves accurate classification of various types of white blood cells including subtypes of lymphocytes.
143. Pirone, D. et al. Identification of drug-resistant cancer cells in flow cytometry combining 3D holographic tomography with machine learning. *Sens. Actuators B* **375**, 132963 (2023).
144. Mirsky, S. K., Barnea, I., Levi, M., Greenspan, H. & Shaked, N. T. Automated analysis of individual sperm cells using stain-free interferometric phase microscopy and machine learning. *Cytom. Part A* **91**, 893–900 (2017).
145. Roitshtain, D. et al. Quantitative phase microscopy spatial signatures of cancer cells. *Cytom. Part A* **91**, 482–493 (2017).
146. Zhang, J. K., He, Y. R., Sobh, N. & Popescu, G. Label-free colorectal cancer screening using deep learning and spatial light interference microscopy (SLIM). *APL Photonics* **5**, 040805 (2020).
147. Wang, H. et al. Early detection and classification of live bacteria using time-lapse coherent imaging and deep learning. *Light Sci. Appl.* **9**, 118 (2020).
148. Ben Baruch, S., Rotman-Nativ, N., Baram, A., Greenspan, H. & Shaked, N. T. Cancer-cell deep-learning classification by integrating quantitative-phase spatial and temporal fluctuations. *Cells* **10**, 3353 (2021).
149. Rotman-Nativ, N. & Shaked, N. T. Live cancer cell classification based on quantitative phase spatial fluctuations and deep learning with a small training set. *Front. Physics* https://doi.org/10.3389/fphy.2021.754897 (2021).
150. Noy, L. et al. Sperm-cell DNA fragmentation prediction using label-free quantitative phase imaging and deep learning. *Cytometry A* **103**, 470–478 (2022).
151. Liu, T. et al. Rapid and stain-free quantification of viral plaque via lens-free holography and deep learning. *Nat. Biomed. Eng* **7**, 1040–1052 (2023).
152. Rivenson, Y. et al. PhaseStain: the digital staining of label-free quantitative phase microscopy images using deep learning. *Light Sci. Appl.* **8**, 23 (2019).
A key study of virtual staining of label-free QPI images of tissue slides using deep learning. Deep learning enabled the automatic transformation of label-free phase images of tissue slides into stained images, eliminating the need for chemical staining.
153. Wang, R. et al. Virtual brightfield and fluorescence staining for Fourier ptychography via unsupervised deep learning. *Opt. Lett.* **45**, 5405–5408 (2020).
154. Nygate, Y. N. et al. Holographic virtual staining of individual biological cells. *Proc. Natl Acad. Sci. USA* **117**, 9223–9231 (2020).
An early study on virtual staining of label-free QPI images of sperm cells using deep learning. By transforming label-free phase images into histochemically labeled images, the study achieves virtual staining of the nucleus and other structures, facilitating rapid evaluation of the quality of individual sperm cells.
155. Ben-Yehuda, K. et al. Simultaneous morphology, motility, and fragmentation analysis of live individual sperm cells for male fertility evaluation. *Adv. Intell. Syst.* **4**, 2100200 (2022).
156. Guo, S.-M. et al. Revealing architectural order with quantitative label-free imaging and deep learning. *Elife* **9**, e55502 (2020).
157. Abdar, M. et al. A review of uncertainty quantification in deep learning: techniques, applications and challenges. *Inf. Fusion* **76**, 243–297 (2021).

158. Angelopoulos, A. N. et al. Image-to-image regression with distribution-free uncertainty quantification and applications in imaging. In Proc. *39th International Conference on Machine Learning*, **162**, 717–730 (2022).
159. Borhani, N., Kakkava, E., Moser, C. & Psaltis, D. Learning to see through multimode fibers. *Optica* **5**, 960–966 (2018).
160. Li, S., Deng, M., Lee, J., Sinha, A. & Barbastathis, G. Imaging through glass diffusers using densely connected convolutional networks. *Optica* **5**, 803–813 (2018).
161. Li, Y., Xue, Y. & Tian, L. Deep speckle correlation: a deep learning approach toward scalable imaging through scattering media. *Optica* **5**, 1181–1190 (2018).
162. Kang, I., Pang, S., Zhang, Q., Fang, N. & Barbastathis, G. Recurrent neural network reveals transparent objects through scattering media. *Opt. Express* **29**, 5316–5326 (2021).
163. Kang, I., Goy, A. & Barbastathis, G. Dynamical machine learning volumetric reconstruction of objects' interiors from limited angular views. *Light Sci. Appl.* **10**, 74 (2021).
164. Kellman, M. R., Bostan, E., Repina, N. A. & Waller, L. Physics-based learned design: optimized coded-illumination for quantitative phase imaging. *IEEE Trans. Comput. Imaging* **5**, 344–353 (2019).
165. Cheng, Y. F. et al. Illumination pattern design with deep learning for single-shot Fourier ptychographic microscopy. *Opt. Express* **27**, 644–656 (2019).
166. Kim, K., Konda, P. C., Cooke, C. L., Appel, R. & Horstmeyer, R. Multi-element microscope optimization by a learned sensing network with composite physical layers. *Opt. Lett.* **45**, 5684–5687 (2020).
167. Mengu, D. & Ozcan, A. All-optical phase recovery: diffractive computing for quantitative phase Imaging. *Adv. Opt. Mater.* **10**, 2200281 (2022).
168. Lin, X. et al. All-optical machine learning using diffractive deep neural networks. *Science* **361**, 1004–1008 (2018).
169. Mengu, D., Luo, Y., Rivenson, Y. & Ozcan, A. Analysis of diffractive optical neural networks and their integration with electronic neural networks. *IEEE J. Sel. Top. Quantum Electron.* **26**, 3700114 (2020).
170. Li, J. et al. Spectrally encoded single-pixel machine vision using diffractive networks. *Sci. Adv.* **7**, eabd7690 (2021).
171. Sakib Rahman, M. S. & Ozcan, A. Computer-free, all-optical reconstruction of holograms using diffractive networks. *ACS Photonics* **8**, 3375–3384 (2021).
172. Yan, H. et al. Virtual optofluidic time-stretch quantitative phase imaging. *APL Photonics* **5**, 046103 (2020).
173. Lee, K. C. et al. Quantitative phase imaging flow cytometry for ultra-large-scale single-cell biophysical phenotyping. *Cytometry A* **95**, 510–520 (2019).
174. Rodenburg, J. & Maiden, A. Ptychography. in *Springer Handbook of Microscopy* (eds. P. W. Hawkes & J. C. H. Spence) 819–904 (Springer, 2019).
175. Park, C., Lee, K., Baek, Y. & Park, Y. Low-coherence optical diffraction tomography using a ferroelectric liquid crystal spatial light modulator. *Opt. Express* **28**, 39649–39659 (2020).
176. Wu, J.-L. et al. Ultrafast laser-scanning time-stretch imaging at visible wavelengths. *Light Sci. Appl.* **6**, e16196 (2017).
177. Lai, Q. T. K. et al. High-speed laser-scanning biological microscopy using FACED. *Nat. Protoc.* **16**, 4227–4264 (2021).
178. Yip, G. G. K. et al. Multimodal FACED imaging for large-scale single-cell morphological profiling. *APL Photonics* **6**, 070801 (2021).

Acknowledgements

This work was supported by the National Research Foundation of Korea (2015R1A3A2066550, 2022M3H4A1A02074314, RS-2023-00241278), an Institute of Information & Communications Technology Planning & Evaluation (IITP; 2021-0-00745) grant funded by the Korea government (MSIT), a KAIST Institute of Technology Value Creation, Industry Liaison Center (G-CORE Project) grant funded by MSIT (N11230131), the Korea Health Technology R&D Project through the Korea Health Industry Development Institute (KHIDI), funded by the Ministry of Health & Welfare, Korea (HI21C0977, HR22C1605), the US National Science Foundation (NSF) Biophotonics Program, NSF PATHS-UP Engineering Research Center and Koç Group.

Competing interests

D.H.R., M.J.L., D.R., H.-s.M. and Y.K.P. have financial interests in Tomocube, a company that commercializes holotomography and quantitative phase imaging instruments. A.O. has financial interests in Lucendi and Pictor Labs, companies that commercialize deep learning-enhanced microscopy and sensing systems for water quality and pathology applications, respectively. All other authors declare no competing interests.

Additional information

Correspondence should be addressed to Aydogan Ozcan or YongKeun Park.

Peer review information *Nature Methods* thanks Keisuke Goda, Jianglei Di and the other, anonymous, reviewer(s) for their contribution to the peer review of this work. Primary Handling Editor: Rita Strack, in collaboration with the *Nature Methods* team.